TRANSACTIONS OF THE INSTITUTE OF FLUID-FLOW MACHINERY

No. 132, 2016, 87–101

Mateusz Grzelczak[1], Adam Tralewski and Zbigniew Pałucki

Analysis of flow structure and performance of the centrifugal compressor impellers

Poznan University of Technology, Chair of Thermal Engineering, Maria Skłodowska-Curie Square 5, 60-965 Poznan, Poland

Abstract

The presently applied desulfurization technologies require a supply of air through centrifugal compressors realizing the pressure increment on the level of 150–200 kPa. Taking the necessary mass flow rate of the processed air into account it is necessary to increase the efficiency of the compression process realized in these machines. The paper will include the results of the works related to the analysis of the gas flow in the compression stage operating with two impellers. The first one has been described with a mathematical function preserving the condition of ruled surface and the geometry of the other impeller has been modeled according to the shape of the meridional velocity profile in the inlet section thus forming leading edge. The common feature of both impellers is the same mathematical function that describes the meridional section and the profile of the blade. The outer diameter of each of the impellers is 200 mm and the blade angle in the outlet section 45°. The compression stage reaches the pressure ratio of 1.4 at the nominal mass flow of 0.73 kg/s maintaining the impeller rotational speed on the level of 24 400 rpm. For the evaluation of the operating parameters and the nature of the gas flow in the compression stage operating with two impellers computational fluid dynamics simulations were carried out and experimental research has been performed using laser Doppler anemometry for impeller of ruled surface.

Keywords: Centrifugal compressors; Cross-section of the rotor; Velocity fluctuation; Tangential/meridional velocity; comppressor impellers

[1]Corresponding Author. Email adress: mateusz.grzelczak@put.poznan.pl

1 Introduction

The requirements related to quality of the products of combustion generated when producing electrical energy in conventional power stations force the manufacturers of power generating machines and equipment to continuously improve the exhaust desulfurization systems.

Issues connected with flow of real fluid through geometrically diversified channels of flow machines raise a lot of questions. The questions relate to correctness and effectiveness of methods facilitating measurement of the fluid flow velocity, verification of the obtained results as well as analyses of measurement errors. One of the methods of measurement of fluid flow velocity is laser Doppler anemometry (LDA). In this case, it was used for measurement of velocity of gas (air) flow through the stage of the blower.

Worldwide experimental tests of the structure of gas flow in centrifugal compressors [1,2,5,6], are aimed at verification of geometry of the stage of a centrifugal impeller in order to obtain high efficiency of the compression process within a wide range of operation of the machine. Due to the high level of diversification of geometries of flow channels in centrifugal impellers of compressors and in order to achieve the above-mentioned target, one has to optimize the shape of meridional cross-section and geometry of the blade to blade channel, which is very often described by complex mathematical functions. A scientist dealing comprehensively with testing of the flow structure in centrifugal compressors with the use of laser anemometry was H. Krain, who presented his results in his study [7].

The research works presented in this paper are related to the analysis of the structure of the gas flow in the compressor impellers based on experimental research using LDA and numerical calculations based on commercial computational fluid dynamics (CDF) software. The aim of the project was to propose a new geometry of the impeller, thus obtaining high isentropic efficiency of the compression process. Based on the performed calculations the authors evaluated the spatial modeling of the impeller blades described with the Gauss curves enabling a full mapping of the meridional velocity profile in the inlet of the impeller. The generated asymmetry of the meridional velocity profile in the inlet cross-section of the impeller is a result of the curvature of the impeller channel in the meridional cross-section that changes the direction of the flow from axial to radial and the geometry of the cap and inlet confusor.

2 Test rig

The rotor geometry is presented in Fig. 2. The basic dimensions and nominal parameters of operation of the blower are presented in the Tab. 1.

Figure 1: Test rig.

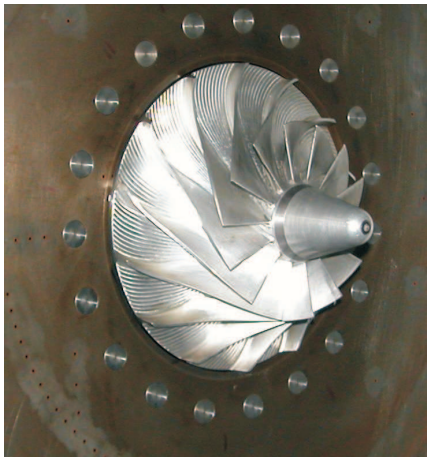

Figure 2: Impeller geometry.

Table 1: Basic geometrical parameters and rotor operating parameters.

Parameters	Symbol	Unit	Value
diameter of the rotor in the inlet at the hub	D_{1h}	mm	50
diameter of the rotor in the inlet at tip	D_{1t}	mm	123.5
diameter of the rotor in the outlet cross-section	D_2	mm	200
width of the rotor at the outlet	b_2	mm	12
blade angle in the inlet at the hub	β_{1h}	deg	25.8
blade angle in the inlet at the tip	β_{1t}	deg	50.4
blade angle in the outlet cross-section of the rotor	β_2	deg	45
number of blades	z	–	14
shaft speed	n	rpm	24400
mass flow rate	q_m	kg/s	0.71
pressure ratio	π	–	1.4

Figure 3 presents operating parameters of a stage of the blower in the form of characteristics. The presented curves show total/total pressure rise of the stage,

Δp_c, characteristics of polytropic efficiency, η_n, and internal power of the compression process, P_i. The above-mentioned parameters were presented as a function of mass flow rate, q_m.

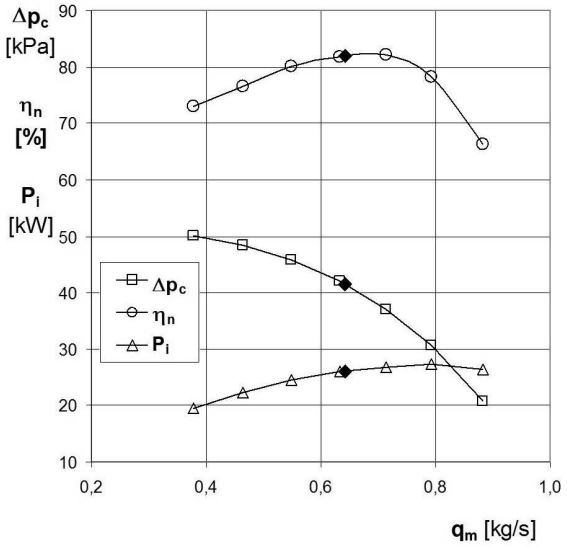

Figure 3: Basic characteristics of operation of the blower.

Before proceeding to main research work involving measurement of velocities of gas flow through the compressor rotor, basic measurements were made. On the basis of operating parameters of the stage, mass flow rate was selected, for which detailed tests were made (Fig. 3). The cross-sections corresponding to measurements of flow velocities were marked with Arabic numerals from 0 to 2. The cross-section 0–0 was located at the distance of $x_1 = 37$ mm from the inlet cross-section of the rotor, cross-section 1–1 at the distance of $x_2 = 2.7$ mm from the same cross-section and cross-section 2–2 at the distance of $x_3 = 1.5$ mm from the outlet cross-section of the rotor. Because of the adopted geometry of the inlet part of the vaneless diffuser in the form of conical surface on the shroud side, the cross-section 2–2 was inclined at the angle of 8.5° (Fig. 4).

3 Experimental results

The measurement results are shown in two ways. First, averaged profiles of flow velocities and profiles of the root mean square (RMS) velocity fluctuation along the height of the rotor blades were presented and, next, velocity fields were pre-

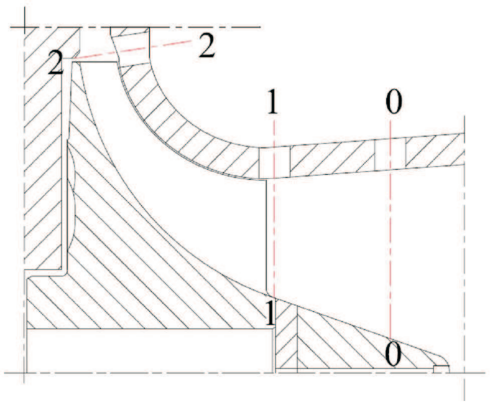

Figure 4: The meridional cross-section of the stage in consideration of measurement points.

sented. Presentation of velocities fields is justified only in the case of the cross-section 1–1 and 2–2, as in these cross-sections we may observe distribution of velocities in relation to width of blade to blade channels. It was observed that there is no reverse influence of the flow upon the distance of 37 mm from the rotor and, therefore, in the cross-section 0–0 the velocity of flow was averaged and the flow was treated as an axisymmetrical flow.

Analyzing the measurement results presented in Fig. 5 and showing the profile of meridional velocity, we may observe asymmetry of the profile with a tendency of occurrence of maximum velocity at a relative height of $h/h_0 = 0.75$. The existing asymmetry results from the suggested geometry of the cap and inlet confusor as well as reverse influence of the flow due to the adopted curvature of the rotor channel in the meridional cross-section. Figure 5 additionally presents the RMS velocity fluctuation, which does not exceed $RMS = 1.2$ m/s at the entire height of the channel, except for layers at the wall.

The meridional velocity in the cross-section 1–1 has an analogous distribution to the cross-section 0–0. The maximum velocity also occurs in the relative height of the blade to blade channel of the rotor – $h/h_0 = 0.75$, however, we may observe higher velocity gradients both on the side of the hub and the shroud. As it has already been mentioned, the existence of such a considerable asymmetry in the flow is caused by curvature of the rotor channel in the meridional cross-section. In the same cross-section (1–1), the RMS velocity fluctuation in the entire range exceeds the value of 5 m/s (Fig. 6) and is considerably greater than the velocity of fluctuation in the cross-section 0–0. The increase of the RMS value is caused

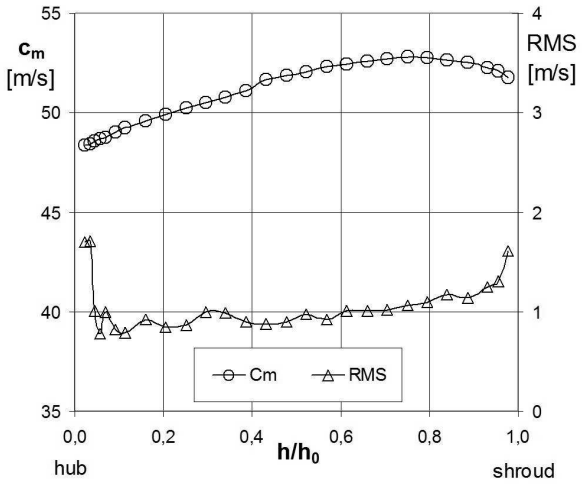

Figure 5: The profile of meridional velocity cm and profile of the RMS velocity fluctuation in the cross-section 0–0.

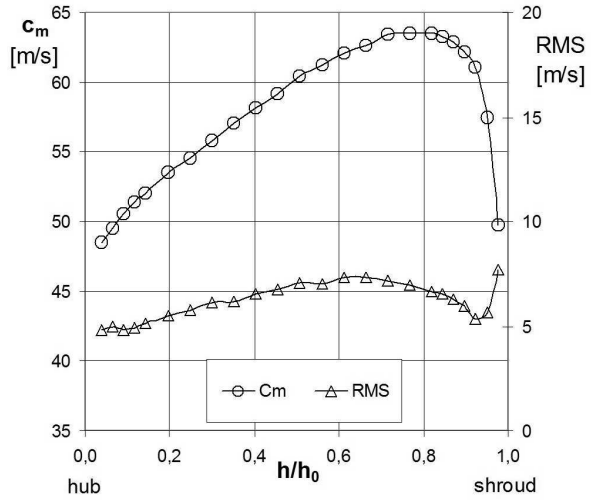

Figure 6: The profile of meridional velocity, c_m, and profile of the RMS velocity fluctuation in the cross-section 1–1.

by reverse influence of the blades upon the flow.

The last cross-section, for which results of measurement of meridional and tangential velocity were obtained is the outlet cross-section of the rotor. In this cross-section, by analyzing first the profile of meridional velocity and averaged

fluctuation of the velocity constituent (Fig. 7), we may observe asymmetry of the profile resulting from occurrence of a summit leakage in the flow through the rotor and intensive growth of boundary layers, which, as a result, lead to formation of a spatial whirl referred to as a 'wake'. The decreased value of meridional velocity on the side of the shroud is also caused by curvature of the channel, i.e., the passage from the axial inlet cross-section to the radial outlet cross-section. The observed character of gas (air) flow on the side of the shroud is also caused by the too large distance of b_2, set up at the design stage. This means that the rotor does not operate in the nominal point. From the results obtained it may be concluded that the maximum value of efficiency occurs for a greater mass flow rate.

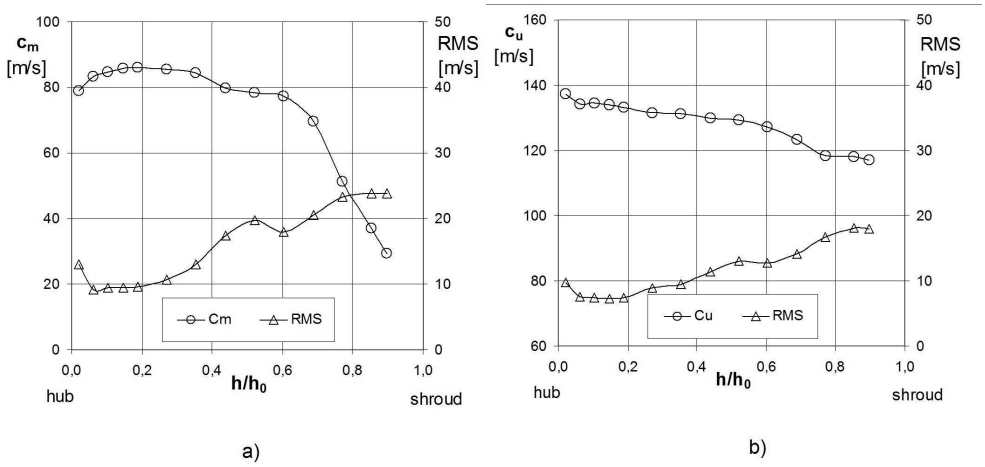

Figure 7: The profile of meridional velocity, c_m, and tangential velocity, c_u, and profile of the RMS velocity fluctuation in the cross-section 2–2

The important information based upon the results obtained is the profile of the RMS velocity fluctuation, more exactly, successive growth of the RMS velocity fluctuation in the direction of the shroud. The observed growth relates both to meridional and tangential velocity. On the side of the hub, RMS of the radial and circumferential constituent of absolute velocity does not exceed 10 m/s (Fig. 7) and on the side of the shroud it is 24 m/s for RMS of the radial constituent and 18 m/s for the circumferential constituent.

The velocity measurements made with the use of laser Doppler anemometry cooperating with marker of the angle identifying location of the rotor blades are presented in this study in the form of fields of velocity. The above-mentioned fields of velocity presented in Figs. 8 to 11 were obtained on the basis of velocity profiles in relation to the blade to blade marker of the rotor.

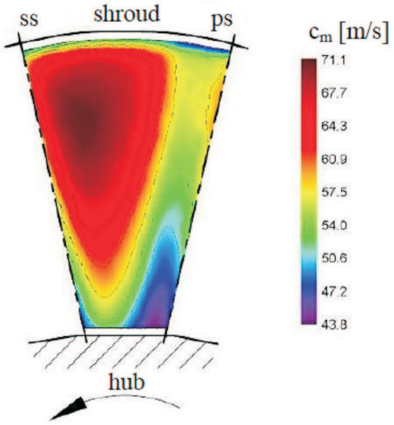

Figure 8: The field of meridional velocity in the inlet cross-section of the rotor (1–1).

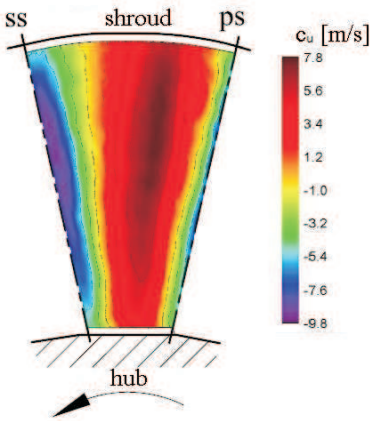

Figure 9: The field of tangential velocity in the inlet cross-section of the rotor (1–1).

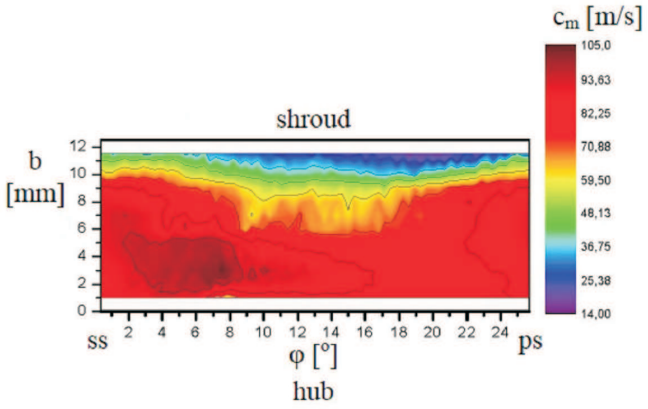

Figure 10: The field of meridional velocity in the outlet cross-section of the rotor (2–2).

Analyzing the fields of velocities in Fig. 8, in the inlet cross-section for meridional velocity we may observe shifting of the maximum velocity area in the direction of the suction side of the blade and the maximum value of that velocity is 70 m/s. On the pressure side of the blade we observe visible minimum velocity.

In the case of tangential velocity in the inlet cross-section along height of the rotor blades, velocity oscillated from the maximum value of 10 m/s to the minimum value of -8 m/s (Fig. 9). This considerable change of velocity is caused exclusively by influence of the leading edge of the rotor blades. This means that

flow onto the rotor in relation to width of the blade to blade channel changes from a backward flow in the area of the rotor blade to a concurrent flow at the half of the channel width.

Figure 10 presents a field of meridional velocity in the outlet cross-section, for which maximum velocity of 95 m/s occupies the area on the side of the suction side of the blade and hub of the rotor. On the side of the shroud, there is a visible decrease in the meridional velocity as well as circumferential velocity (Fig. 11). The area of decreased velocity is particularly visible in the half of the width of the blade to blade channel.

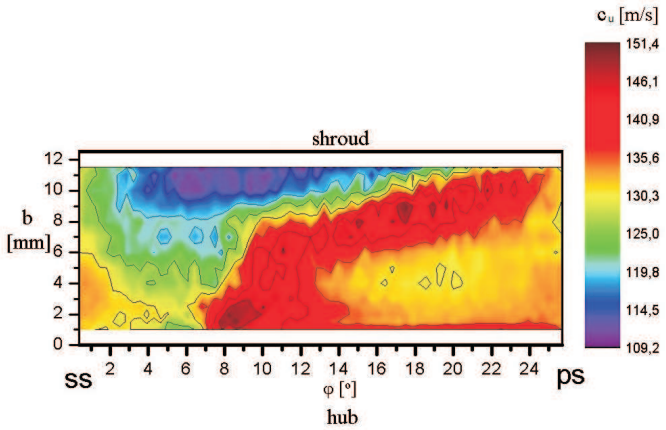

Figure 11: The field of tangential velocity in the outlet cross-section of the rotor (2–2).

4 New impeller blade design

Modeling of the leading edge in centrifugal compressor impellers is very often based on one-dimensional methods that assume a constant value of the absolute velocity along the height, r, of the blade $c_m(r) = const$. The main assumption that makes the manufacturing of the impeller is easier is that the blade geometry fulfilling the ruled surface condition as this condition has a positive impact on the impeller production through machining. However, taking into account the one-dimensional model of the flow and assuming the ruled surface condition increases the occurrence of divergence in the angle of the gas flow and the blade angle, which frequently leads to a drop in the compressor efficiency.

Based on the conducted research the paper presents the velocity profile in the inlet cross-section of the impeller (Fig. 6) that subsequently leads to the determination of the profile changes of the β_1 flow angle along the height of the blade.

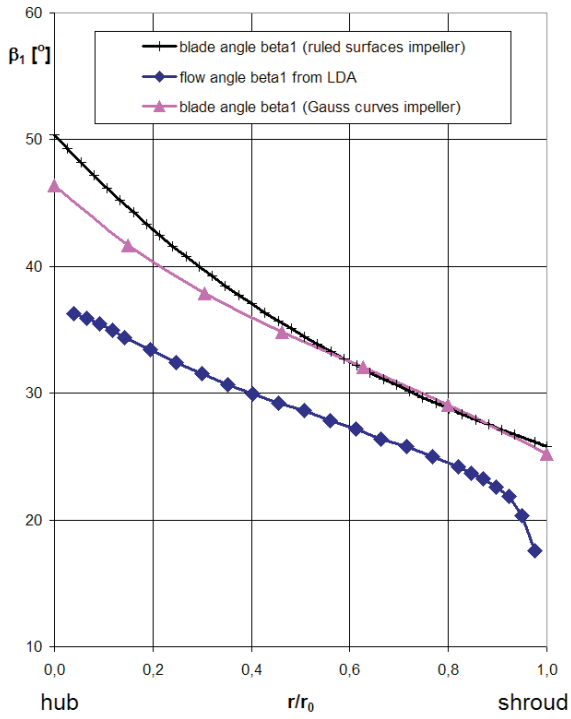

Figure 12: Radial distribution of flow and blade angle β_1.

Comparing the obtained angle of flow with the blade angle (Fig. 12) a significant influence has been observed of the asymmetric velocity profile on the β_1 flow angle and on the deviation of this angle from the blade angle near the hub and the shroud of the impeller. Positive angles of attack in these areas assume values above 10°. The existing situation contributes to the occurrence of impact losses that reduce the impeller efficiency. In order to minimize these losses new impeller geometry was proposed that provides for the mapping of the velocity profile on the leading edge of the blade. The conducted mapping consisted in a creation of seven blade profiles distributed proportionally along the blade height. Each of the profiles in the inlet provided for the local value of the meridional velocity obtained in the measurements. In such a way an impeller was formed whose geometry we can see in Fig. 13 The geometry of the presented impeller was developed including the durability conditions of used material. This means that the velocity profile obtained based on the measurements at a distance of 2.7 mm from the impeller

inlet cross-section (1–1) was unacceptable due to a strong deflection of the blade tips in the inlet cross-section. The adopted compromise consisted in forming of the blade described with the Gauss curvature based on the velocity profile from the 0-0 cross-section (Fig. 5). The above-presented geometry resulted from the conducted strength analyses. As for the impeller modeled based on the velocity profile from the 1–1 cross-section these analyses have shown an excess of the admissible tensions on the blade tips caused by the centrifugal force.

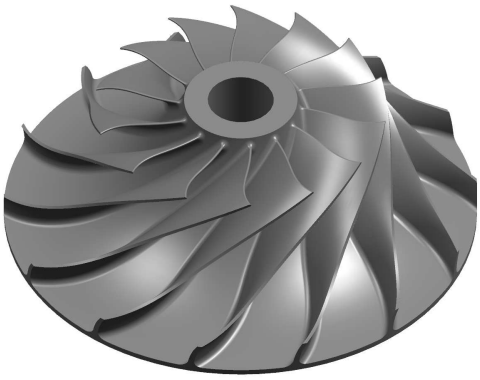

Figure 13: The impeller geometry described with the Gauss curvature

5 Results of computational fluid dynamics simulations

This section contains the comparison of the thermodynamic and flow quantities of the above-presented impellers. The said quantities were obtained based on numerical calculations carried out with commercial computational fluid dynamics software, namely ANSYS CFX 13.0 numerical code.

The analysis of the results consisted in interpreting of the meridional velocity fields for five control cross-sections of the impellers (Fig. 14). The position coordinates of control cross-section 1 and 5 were related to the probing coordinates of the meridional velocity using LDA for the impeller preserving the ruled surface condition. The compared geometries of the impellers are different in the shape of the leading edge of the blades. The other geometrical parameters are the same. Additionally, for the calculations, the same values representing the boundary conditions have been assumed.

The velocity fields in the 1–1 cross section (Fig. 15) for each impeller are

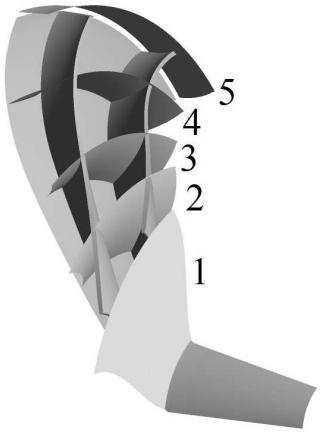

Figure 14: Calculated cross sections for the impeller

characterized by an asymmetric distribution of velocities along the height of the blade and a drop in the meridional velocity in the area where the leading edge of the impeller is present. The obtained results of the calculations are analogical to the velocity fields obtained in the LDA measurements. In the 2–2 cross-section (Fig. 15) we can observe that the application of the blades described with the Gauss curvature is purposeful (compared to the developable blade surfaces). The differences between the presented results for each of the impellers are visible particularly from the suction side of the blade. In the case of the developable impeller a separation has been located due to wide angles of attack, hence we can observe a region of reduced meridional velocity at the tip of the blade. The velocity fields obtained for the impeller described with the Gauss curvature do not have any separation in the suction side of the blade. In this area we can only see a boundary layer of a constant thickness.

Another advantage of the new impeller is a reduced area of lower velocity generated by the blade tip leakage. The reason for such a situation is the deflection of the tip in the direction of the impeller rotation.

In the 3–3 cross-section (Fig. 15) we can still see the influence of the leading edge on the flow in the suction side of the blade and the shroud (reduced meridional velocity). An unwanted flow phenomenon for each of the impellers is the reduced velocity on the pressure side of the blade near the shroud of the impeller, yet this area is greater for the impeller maintaining the ruled surface condition.

Important information directly influencing the evaluation of the radial im-

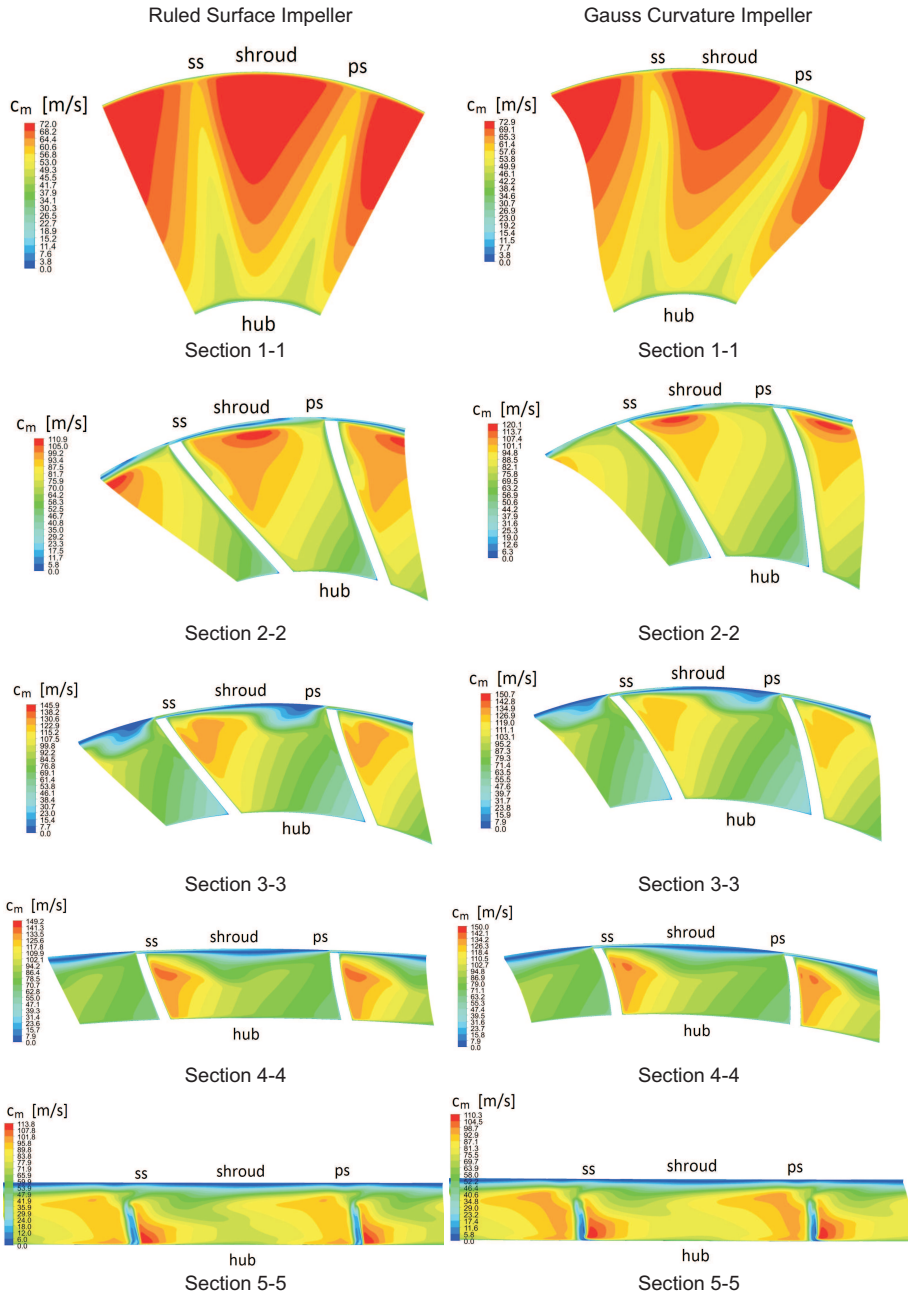

Figure 15: Comparison of meridional velocity distribution at five sections for the ruled surface impeller and Gauss curvature impeller.

peller operation in centrifugal blower is the value of the wake and the values of the velocity in this area. These gradients have a direct impact on the energy dissipation and, hence, the drop in the politropic efficiency of the blower. In the 5–5 cross-section (Fig. 15) of the new impeller we can see a wake of lower intensity, which analogically, leads to maintaining of a lower rise of entropy in the flow.

The quantitative comparison of the thermodynamic and flow parameters of each of the impellers is a complement of the obtained results. To this end a table was created in which the basic physical quantities that characterize the centrifugal compressors have been specified: the rise of the total pressure, isentropic efficiency. The results of the calculations have been presented in Tab. 2.

Table 2: The results of calculations.

Parameter	Symbol	Unit	Value	
			Ruled surface impeller	Gauss curvature impeller
Pressure rise	Δp_c	kPa	41.45	41.76
Total isentropic stage efficiency	η_{stt}	%	91.7	92.3

6 Conclusions

Based on the conducted research and numerical calculations for the presented geometries of the impeller we can conclude that application of blades described with the Gauss curvature is more justified than the ones preserving the ruled surface condition. The advantage of such an impeller is greater isentropic efficiency at a mere several percent increase in the production costs through CNC machining.

The authors of the paper imply that the proposed impeller modeling is appropriate particularly for centrifugal blowers characterized by high specific speed value and ratio b_2/D_2 above 6%. These work indexes are used in blowers for air supply systems such as flue exhaust gases desulfurization systems or waste water treatment where pressure ratio should not exceed $\pi = 2.5$.

The above implication results from the need to apply sufficiently high blades in the axial section in impellers of a relative width in the range of b_2/D_2 from 6 to 8%. Such a solution forces the application of small radiuses of the shroud, which results in a growth of the flow losses. If, additionally in the flow near the shroud the detachment occurs resulting from high angles of attack at the blade tips will certainly increase the flow losses in this area.

The assumed shape of the leading edge presented in the paper resulted in a reduction of the impact losses caused by the stream separation in the inlet of the impeller channels, which allowed greater isentropic efficiency of the compressing stage.

Acknowledgment Experimental tests were conducted with the use of a prototype centrifugal blower equipped with a semiopen impeller (Fig. 1) The rotor geometry was created as a result of comprehensive design works and numerical analyses conducted under the project entitled 'Development of optimum structures of series of types of compressors and high power radial blowers' financed by the European Regional Development Fund, POIG and carried out in collaboration with a manufacturer of mechanical equipment H. Cegielski Poznań S.A.

Received 29 November 2013

References

[1] Eckardt D.: *Detailed flow investigation with in a high – speed centifugal compressor impeller.* J. Fluids Eng.-T. ASME **98**(1976), 390–402.

[2] Eisenlohr G., Krain H., Richter F. A., Tiede V.: *Investigations of the flow through a high pressure ratio centrifugal impeller.* ASME (2002), GT-2002-30394.

[3] Grzelczak M.: *Analysis of the flow of gas in a compressor impeller on the basis of velocity measurements with the use of LDA laser anemometer.* In: Proc. Int. Conf. SYMCOM'11, Turbomachinery, Łódź 2011.

[4] Grzelczak M.: *The influence of the impeller inlet blades on the efficiency of the blower.* In: Proc. Int. Conf. SYMCOM'11, Turbomachinery, Łódź 2011.

[5] Higashimori H., Hasagawa K., Sumida K., Suita T.: *Detailed flow study of mach number 1.6 high transonic flow with a shock wave in a pressure ratio 11 centrifugal compressor impeller.* ASME (2004), 2004-GT-53435.

[6] Japikse D.: *Centrifugal Compressor Design and Performance.* Berlin, Sept. 24–28, **2**(1990), 4–16.

[7] Krain H., Karpinski G., Beversdorff M.: *Flow analysis in a transonic centrifugal compressor rotor using 3-component laser velocimetry.* ASME (2001), 2001-GT-315.